

Bovine heart cytochrome oxidase was isolated and the CO complex prepared by procedures reported elsewhere.^{8,15} The apparatus used was similar to the one described previously for our TRIR experiments.⁸ It is based upon photodissociation by laser pulses at 532 nm (7-ns duration, 10-Hz repetition rate) and infrared probing with a CW tunable diode laser. CaF_2 was substituted for sapphire optics, and a half-wave plate in the YAG beam allowed polarization vector orientation. Infrared transient signals (typically 2000 averaged transients) were recorded as a function of YAG vs IR E-vector orientation and also as a function of photodissociation fraction (f) between 10% and 67%. Values of α were determined from the equation $R = [4 - \langle \sin^2 \alpha \rangle] / [2 + 2 \langle \sin^2 \alpha \rangle]$,¹² with a value of $R(t=0)$ obtained by linear extrapolation to $f = 0$. The preceding equation assumes x, y degeneracy of the heme absorbance at 532 nm.

Figure 1a shows typical results of the TRIR experiments for heme-CO (1963 cm^{-1}) and Cu-CO (2061 cm^{-1}). The heme-CO data show the transient over the first 30 μs after photodissociation, during which period the recombination of CO with the heme is negligible.¹⁵ The results for Cu_B^+ -CO are similar except that the Cu-CO transmittance transient, which is formed in less than 200 ns,⁸ is negative rather than positive and persists only for a few microseconds, the lifetime of the Cu_B^+ -CO complex.⁸ Transient linear dichroism is clearly evident in the Fe-CO results; the short-time bleaching at $\theta = 90^\circ$ is substantially greater than at $\theta = 0^\circ$. The dichroism disappears with time as a consequence of rotational diffusion of the protein, with a half-life of approximately 6 μs under these conditions ($T = 300\text{ K}$, 1 mM CcO, 50% glycerol solution).

Figure 1b shows the dependence of the Fe-CO infrared polarization ratio upon time at $f = 30\%$. These data were measured at various values of f and extrapolated to $f = 0$, yielding $R = 1.71$ for heme-bound CO, whence $\alpha = 21^\circ (\pm 2^\circ)$. For Cu_B^+ -CO, $R = 1.07$ and $\alpha = 51^\circ (\pm 3^\circ)$. These conclusions are model-dependent. For heme-CO, a discrete value of α is assumed rather than a distribution of angles.¹⁰ This should be a good assumption for CcO in particular, because its CO IR peak is more narrow than that of any heme-CO protein examined to date (the C-O stretching frequency is sensitive to α ; therefore a distribution in α leads to inhomogeneous broadening of the CO IR peak: see, for example, ref 5 and 12). The same assumption is made for Cu_B^+ -CO with the same justification; the narrow line width of the copper-bound C-O stretch is good evidence that CO is not randomly oriented, despite almost isotropic linear dichroism, but instead is oriented at nearly the "magic angle" to the heme normal. In addition, it is assumed that the C-O axis of Cu-CO is approximately coplanar with the heme normal.

A number of workers have noted an empirical correlation between the frequency of the C-O stretch in CO-hemes and constraints that force the ligand to be oriented off the normal to the heme plane.¹⁶⁻¹⁸ These constraints may "bend" the Fe-C-O angle away from 180° , or "tilt" the Fe-C-O structure as a unit away from the heme normal, or both. A high CO frequency has been taken as an indication that the CO is more nearly upright. In view of this, it has often been presumed that the high C-O frequency in CcO suggests that the ligand is nearly perpendicular to the heme plane. Our measurements indicate that CcO-CO ($\nu_{\text{CO}} = 1963\text{ cm}^{-1}$) has $\alpha = 21^\circ$, almost the same as the 1944-cm^{-1} MbCO conformer (20° at 300 K) and HbCO (18° , 1951 cm^{-1}).¹²

The value of α is the sum of the bend and tilt angles, assuming that the two distortions are in the same plane. Rousseau and co-workers²⁰ estimated the bend angle in CcO-CO to be $175^\circ (\pm 5^\circ)$, using equations that have been developed^{17,19} for calculating this quantity from vibrational frequencies. They suggest from other arguments that CO is significantly tilted as well. We can quantitatively test conclusions, given our present work and related results on other proteins. The bend angle of 175° requires a 16° tilt of the Fe-C axis to achieve $\alpha = 21^\circ$. Values of the Fe-C tilt between 10° and 14° have been estimated for HbCO and MbCO;¹² thus our value of α and the calculated bend angle²⁰ are plausibly consistent. The bend angle calculations from vibrational data embody assumptions that limit their general validity and therefore should be viewed with caution.²¹ Nevertheless, it seems clear that the simple correlation of ν_{CO} with either bend angle or α is not valid. MbCO and CcO-CO apparently have very similar values of bend angle (174° , 175°) and α (20° , 21°), yet their ν_{CO} 's differ by 20 cm^{-1} .

The structural interpretation of the α value for Cu_B^+ -CO is not as clear as for the heme because the 51° C-O vector of Cu-CO may point either toward or away from the heme plane, and also toward or away from the heme normal. Cu_B is thought to be 5 Å or less from the heme a_3 iron in CcO,²² but no evidence exists as to its location with respect to the heme normal. Finally, we note that both the heme and Cu_B α values are cone half-angles, and we have no evidence as to the angular orientations of the (Fe)C-O and (Cu)C-O vectors on their respective cone surfaces. Experiments designed to clarify these structural issues are in progress.

Acknowledgment. This work was supported by National Institutes of Health Grant DK36263 (W.H.W.) and performed at The University of California, Los Alamos National Laboratory, under the auspices of the U.S. Department of Energy.

(19) Champion, P. M.; Stallard, B. R.; Wagner, G. C.; Gunsales, I. C. *J. Am. Chem. Soc.* **1982**, *104*, 4345-4351.

(20) Argade, P. V.; Ching, Y. C.; Rousseau, D. L. *Science* **1984**, *225*, 329-331.

(21) López-Garriga, J. J.; Oertling, A. W.; Babcock, G. T.; Woodruff, W. H., manuscript in preparation.

(22) Babcock, G. T. In *Biological Applications of Raman Spectroscopy*, Spiro, T. G., Ed.; Wiley-Interscience: New York, 1988; Vol. 3, p 298.

Ultrafast Studies of Transition-Metal Carbonyl Reactions in the Condensed Phase: Solvation of Coordinatively Unsaturated Pentacarbonyls

M. Lee and C. B. Harris*

Department of Chemistry, University of California
Berkeley, California 94720
Materials and Chemical Sciences Division
Lawrence Berkeley Laboratory
Berkeley, California 94720

Received May 15, 1989

Recently ultrafast studies on the photodissociation dynamics of transition-metal carbonyls have drawn considerable attention.¹ In the gas phase, electronically excited $\text{Cr}(\text{CO})_6$ molecules lose CO, depending on the initial energy content. In liquids, on the other hand, only $\text{Cr}(\text{CO})_6 \rightarrow \text{Cr}(\text{CO})_5 + \text{CO}$ occurs due to fast vibrational relaxation.² A solvent molecule (S) is then expected to enter the vacant metal site of $\text{Cr}(\text{CO})_5$ to form a complex. The absorption spectrum of $\text{Cr}(\text{CO})_5\text{S}$ critically depends on the solvent property as its maximum is known to reflect the bond strength between the metal and the solvent.³ While the absorption maxima

(14) Woodruff, W. H.; Kessler, R. J.; Ferris, N. S.; Dallinger, R. F.; Carter, K. R.; Antalis, T. M.; Palmer, G. In *Electrochemical and Spectrochemical Studies of Biological Redox Components*; Kadish, K. M., Ed.; Advances in Chemistry 201; American Chemical Society: Washington, DC, 1982; pp 625-659.

(15) Elnarsdóttir, Ó.; Killough, P. M.; Dyer, R. B.; López-Garriga, J. J.; Atherton, S. J.; Hubig, S. M.; Palmer, G.; Woodruff, W. H., manuscript in preparation.

(16) Caughey, W. S. In *Methods for Determining Metal Ion Environments in Proteins: Structure and Function of Metalloproteins*; Darnall, D. W., Wilkins, R. G., Eds.; Elsevier/North-Holland: New York, 1980; pp 95-115.

(17) Yu, N.-T.; Kerr, E. A.; Ward, B.; Chang, C. K. *Biochemistry* **1983**, *22*, 4534-4542. Yu, N.-T.; Benko, B.; Kerr, E. A.; Gersonde, K. *Proc. Natl. Acad. Sci. U.S.A.* **1984**, *81*, 5106-5110.

(18) Li, X. Y.; Spiro, T. G. *J. Am. Chem. Soc.* **1988**, *110*, 6024-6032.

(1) See, for example: *Ultrafast Phenomena VI*; Yajima, T., Yoshihara, K., Harris, C. B., Shlonoya, S., Eds.; Springer: Berlin, 1988.

(2) Welch, J. A.; Peters, K. S.; Valda, V. *J. Phys. Chem.* **1982**, *86*, 1941.

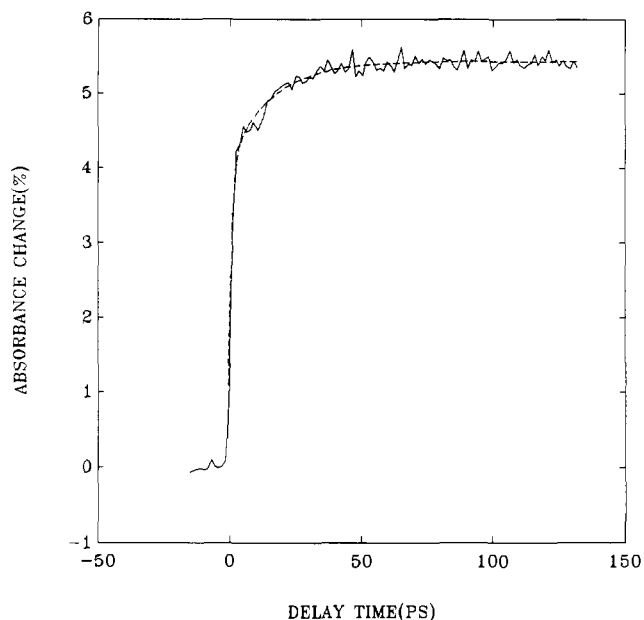


Figure 1. Percent absorbance change of electronically excited $\text{Cr}(\text{CO})_6$ at 295 nm in cyclohexane probed at 500 nm. The dotted line is a non-linear square fit to data: $f(t) = -4.058 \exp(-t/1.1 \text{ ps}) - 1.396 \exp(-t/16.6 \text{ ps}) + 5.454$. The fit was obtained without deconvolution from the instrument function (1 ps) so that the true time constants (especially the short component) should be faster.

of the gas phase⁴ and unsolvated (naked)⁵ $\text{Cr}(\text{CO})_5$ occur around the 620-nm region, they occur at 500 and 450 nm in cyclohexane and THF, respectively,⁶ THF interacting more strongly with Cr than cyclohexane.

Simon and co-workers measured a pulse width limited rise in the transient absorption signal of $\text{Cr}(\text{CO})_5$ in cyclohexane at 500 nm. They concluded that the formation of the solvated complex $\text{Cr}(\text{CO})_5\text{S}$ is complete within less than 1 ps and the stable form of the complex should be a square pyramid.⁷ This interpretation, however, has been questioned by Spears and co-workers, who employed a 20-ps UV pump and infrared probe (CO stretching frequency region) technique.⁸ They claimed that a "naked" $\text{Cr}(\text{CO})_5$ in liquids persisted on a 100-ps time scale. They also argued that there exist two different solvent coordination species for $\text{Cr}(\text{CO})_5\text{S}$: a singlet square pyramid and a triplet trigonal pyramid.

In an attempt to understand the solvation dynamics more fully, we carried out picosecond pump-probe measurements in the visible region with the 1-ps time resolution. The experimental details have been described elsewhere.⁹ Briefly, 1-ps, 100- μJ pulses at 295 nm were used to excite the sample, and transient absorption signals were measured by using 10 nm fwhm bandpass filters at selected probe wavelengths (500–680 nm) from a continuum generated in a water cell. In order to avoid interfering photochemical reactions resulting from the high reactivity of photo-dissociated species, a liquid jet setup was used.

The absorbance change of photoexcited $\text{Cr}(\text{CO})_6$ in cyclohexane at 500 nm is shown in Figure 1. In contradiction to the fast rise (<1 ps) reported by Simon et al., our data having a high signal-to-noise ratio shows a slow rise with a 17-ps time constant. A separate experiment showed that the final signal level does not

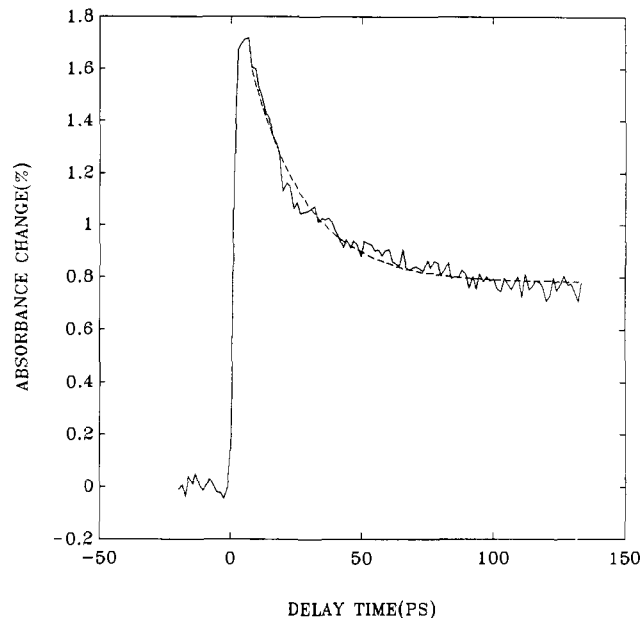


Figure 2. Transient absorption signal of $\text{Cr}(\text{CO})_5$ in cyclohexane at 622 nm. The fit is $f(t) = 0.875 \exp(-t/20.7 \text{ ps}) + 0.786$.

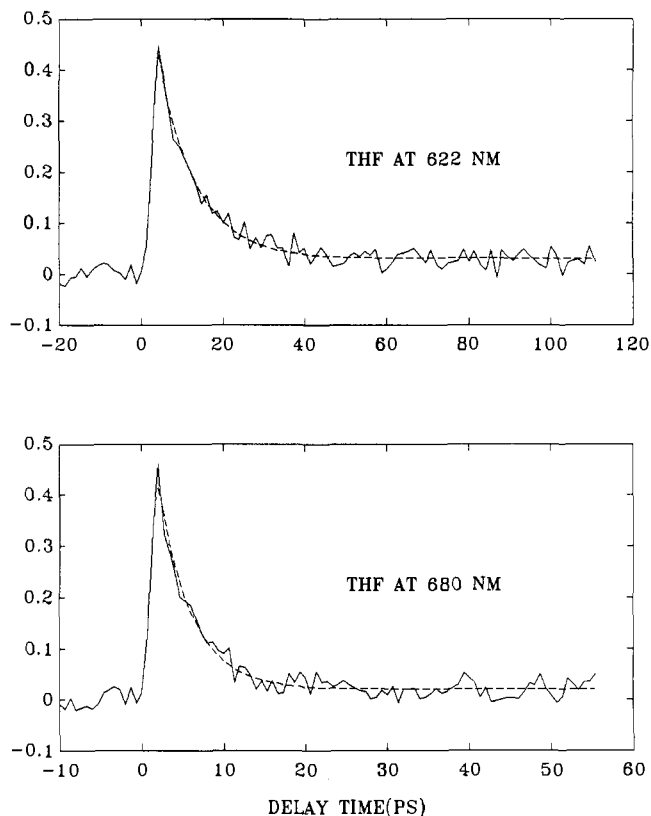


Figure 3. Intermolecular energy dissipation of $\text{Cr}(\text{CO})_5$ molecules dissolved in THF at 622 nm (a) and 680 nm (b). Time constants are (a) 9 ps and (b) 4 ps without deconvolution.

(3) Perutz, R. N.; Turner, J. J. *J. Am. Chem. Soc.* **1975**, *97*, 4791. Burdett, J. K.; Grzybowski, J. M.; Perutz, R. N.; Pollakoff, M.; Turner, J. T.; Turner, R. F. *Inorg. Chem.* **1978**, *17*, 147.

(4) Breckenridge, W. H.; Stewart, G. M. *J. Am. Chem. Soc.* **1986**, *108*, 364.

(5) Kelly, J. M.; Long, C.; Bonneau, R. *J. Phys. Chem.* **1983**, *87*, 3345.

(6) Simon, J. D.; Peters, K. S. *Chem. Phys. Lett.* **1983**, *98*, 53.

(7) Simon, J. D.; Xie, X. *J. Phys. Chem.* **1986**, *90*, 6751; **1987**, *91*, 5538; **1989**, *93*, 291.

(8) Wang, L.; Zhu, X.; Spears, K. G. *J. Am. Chem. Soc.* **1988**, *110*, 8695; *J. Phys. Chem.* **1989**, *93*, 2.

(9) Harris, A. L.; Berg, M.; Harris, C. B. *J. Chem. Phys.* **1986**, *84*, 788.

change up to 1 ns, indicating that the solvent complex is stable on this time scale. To determine whether the 17-ps rise is due to vibrational relaxation, the absorbance change around 620 nm was measured. This wavelength region corresponds to the red tail of the absorption spectrum of solvated $\text{Cr}(\text{CO})_5$ so that the vibrationally hot species with ca. 4000- cm^{-1} excess energy may be observed. Figure 2 shows the absorbance change in cyclohexane at 622 nm. The cyclohexane data clearly show a decay with a 21-ps time constant, which is very close to the rise time at 500 nm. This is faster than the infrared measurement by Spears et al.⁸ We should, however, point out that Spears et al. used 266-nm

pulses for excitation and they may have observed a different initial species.

We also measured the relaxation time of vibrationally hot $\text{Cr}(\text{CO})_5$ in THF at 622 and 680 nm. It was expected that the data at 680 nm would show a faster decay than at 622 nm because, at 680 nm, one probes those molecules that are vibrationally hotter by 1370 cm^{-1} . Indeed, a 9-ps decay at 622 nm and a 4-ps decay at 680 nm were observed (Figure 3). The decay in THF at 622 nm is faster compared to cyclohexane at the same wavelength. This may be because the absorption maximum in THF appears in the bluer region compared with cyclohexane (450 nm for THF and 500 nm for cyclohexane). Therefore, $\text{Cr}(\text{CO})_5(\text{THF})$ is vibrationally hotter (2220 cm^{-1}) than $\text{Cr}(\text{CO})_5(\text{cyclohexane})$ at 622 nm.

Our data indicate that the dynamics for solvation in the highly reactive pentacarbonyls is controlled by the dissipation of the excess vibrational energy to surroundings. The intermolecular energy transfer times of vibrationally hot $\text{Cr}(\text{CO})_5$ in cyclohexane and THF appear to be 4–21 ps for the excess energy of $4000\text{--}7500\text{ cm}^{-1}$, which are faster than T_1 relaxation times of the CO stretching in $\text{Cr}(\text{CO})_6$ in solution as measured by Heilweil et al.¹⁰ Our observation of vibrational cooling, we think, may clarify the issue of the existence of "naked" $\text{Cr}(\text{CO})_5$ in liquids.

Acknowledgment. This work was supported by the Office of Naval Research and the U.S. Army Research Office.

(10) Heilweil, E. J.; Cavanagh, R. R.; Stephenson, J. C. *Chem. Phys. Lett.* 1987, 134, 181; *J. Chem. Phys.* 1988, 89, 230.

Effect of Surface Acoustic Wave Generated on Ferroelectric Support upon Catalysis

Yasunobu Inoue,* Masahiko Matsukawa, and Kazunori Sato

Analysis Center, Nagaoka University of Technology
Nagaoka Nagaoka, Niigata Japan

Received April 17, 1989

The development of a catalyst whose function can be activated by external energy is one of the most interesting subjects. We have directed our attention to the surface acoustic wave (SAW) which can be propagated on ferro- and piezoelectric crystals having no center of symmetry.¹⁻³ Since the wave is able to cause the replacement of lattice atoms and an associated electric field, it would be expected that the SAW possesses the capability of activating a catalytic phase combined with a ferroelectric surface. There have so far been few studies on the effect of the SAW in this respect, and, to our knowledge, this is the first report describing the availability of the SAW for catalysis.

In the present work, a SAW was generated on a ferroelectric LiNbO_3 substrate which had a high piezoelectric coupling coefficient. Palladium was chosen as a catalytically active phase and was deposited as a thin film on the ferroelectric substrate.

A SAW device employed is schematically shown in Figure 1. The interdigital transducer (IDT) electrodes were fabricated photolithographically at each end of a polished single-crystal surface of 128° -rotated Y-cut LiNbO_3 . The electrode for SAW generation had 20 pairs of a double finger with a spacing of $200\text{ }\mu\text{m}$, and the SAW-receiving electrode had the same structure except for 14 pairs. Both the electrodes consisted of a 10-nm underlying Cr layer covered with an inactive 100-nm-thick Au layer. The distance between the SAW generation and detection electrodes was 16 mm, in the middle of which a Pd film was

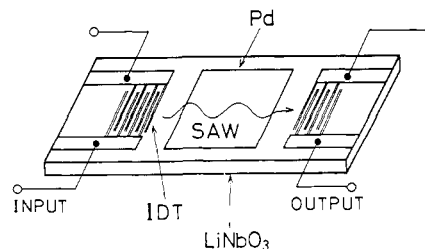


Figure 1. Schematic representation of a SAW catalyst.

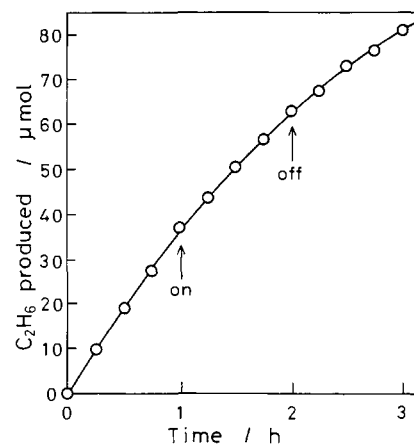


Figure 2. Hydrogenation of C_2H_4 on a SAW catalyst. Initial pressures: 4 kPa of H_2 and C_2H_4 .

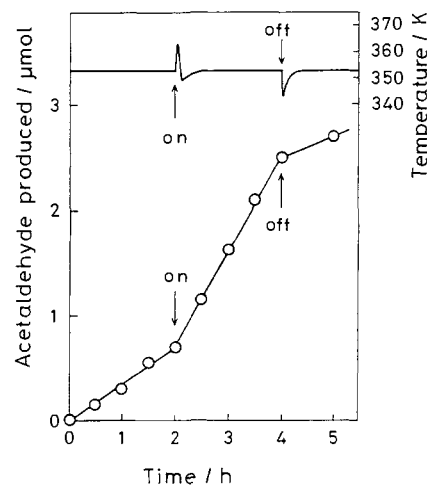


Figure 3. Effect of a SAW upon the catalytic activity of Pd for the formation of acetaldehyde and temperature of the catalyst surface. Initial pressures: 4 kPa of $\text{C}_2\text{H}_5\text{OH}$ and O_2 .

deposited at a thickness of 10 nm by evaporation with resistance heating. Radio frequency (rf) power was generated from a network analyzer, then amplified, and, after adjustments through several attenuators, applied at 1 W. The electric circuit was set up so that the SAW was able to pass through the Pd catalyst and then to return back to the network analyzer.

The gas-phase catalytic reactions were investigated in a high-vacuum circulating system in which the Pd-incorporated SAW catalyst was placed in a quartz reaction cell with the electrodes. The temperature of the catalyst was monitored by a small thermocouple connected directly to the back of the LiNbO_3 substrate and held constant with an outside electric furnace. It was experimentally confirmed that changes in the temperature of the Pd surface were reflected in the back of LiNbO_3 substrate with a delay of ca. 10 s. This delay was negligibly small, compared to the scale of time during which the catalytic reactions were being examined.

The bandpass characteristics of the SAW device showed that the center of the SAW appeared at a frequency of 19.5 MHz and

(1) Auld, B. A. *Acoustic Fields and Waves in Solids*; John Wiley and Sons: New York, 1973; Vol. II, p 163.

(2) White, R. M. *Proc. IEEE* 1970, 58, 1238.

(3) Wohltjen, H.; Dessy, R. *Anal. Chem.* 1979, 51, 1458.